Reaction Kinetics at Polymer−Polymer Interfaces

Ben O'Shaughnessy* and Uday Sawhney

Department of Chemical Engineering, Materials Science and Mining Engineering, Columbia University, New York, New York 10027

Received January 25, 1996; Revised Manuscript Received June 24, 1996[⊗]

ABSTRACT: We present a theoretical study of polymer−polymer reaction kinetics at an interface separating two immiscible polymer phases. Such reactions are widely employed in reactive blending of incompatible species. When functional groups are weakly reactive, the rate constant k obeys mean field theory: $k \propto h$, where h is the interface thickness. For strongly reactive end groups (diffusion-controlled limit) we show that the interface increases the effective dimensionality of the problem by one: reaction rates obey scaling laws as for a 4-dimensional bulk problem. This leads to $k \sim 1/\ln N$ and $k \sim 1/N$ (to within logarithmic factors) for unentangled and entangled melts, respectively, where N is the degree of polymerization. These are quite different from the corresponding scalings for bulk reactions: $k \sim 1/N^{1/2}$ and $k \sim 1/N^{3/2}$. k depends only logarithmically on h for unentangled systems and is independent of h for entangled cases. As the interface becomes crowded with diblock product, k becomes exponentially small when the area per chain, Σ, drops below $N^{1/2}$: $k \sim e^{-\text{const } N/\Sigma^2}$. Consistent with a number of experiments, we conclude that during reactive blending surface tension reduction is minimal and reduced droplet−droplet coalescence rates are dominant.

I. Introduction

A variety of industrial processes involve the chemical reaction of polymers at an interface separating two immiscible polymer phases (see Figure 1). Interfacial polymer reactions are also of fundamental importance as a probe of polymer statics and dynamics at surfaces,[1−4] many aspects of which remain open. However, the present study is motivated principally by industrial applications; of particular commercial relevance for the creation of new materials with enhanced properties is the process of *reactive blending*.[5−8] This frequently provides an attractive alternative to costly developments of new copolymer syntheses. In reactive blending systems the mechanical mixing of two thermodynamically immiscible polymer species A and B is assisted by reactions at interfaces separating droplets of the minority phase A (say) from the continuous B phase (see Figure 2). A certain fraction of A and B chains bear chemically reactive groups which can meet one another in the thin interfacial regions only. The A−B copolymers produced by these reactions, which would be linear A−B diblocks in the case where the reactive groups are at chain ends, can increase interfacial strengths[9−11] and are believed to promote mixing in two ways. First, droplet coalescence rates are reduced through steric repulsion; second, droplet breakup rates are increased through lowered interfacial tension.[12,13] In recent controlled experiments, Sundararaj and Macosko[7] have examined these issues and have suggested that the dominant influence is through suppressed coalescence rates. They observed significantly smaller droplets when copolymers were created in situ by reactions than when presynthesized diblocks or triblocks were added. Other experimental studies suggest a similar picture;[6,8] shown in Figure 4 are the measurements of Okamoto and Inoue[6] who find smaller droplets for higher concentrations of coupling agent, i.e. when the functional groups have, in effect, greater reactivity.

A number of basic questions are begged. How rapidly do copolymers build up at the interface? How does this rate depend on functional group reactivity, on properties of the interface such as its thickness, on the polymer molecular weights and on the density of copolymers as they accumulate and crowd up the interface? On the theoretical side, many of the same questions for the closely related problem of *small* molecule interfacial reactions have been examined in an earlier study;[14] much of what follows builds on that work. A short version of the present manuscript has already appeared.[15] An independent theoretical study addressing the same situation as that studied here, namely end-functionalized polymers reacting at an interface, has also recently appeared.[16] A number of conclusions of that work and the present paper are in common.

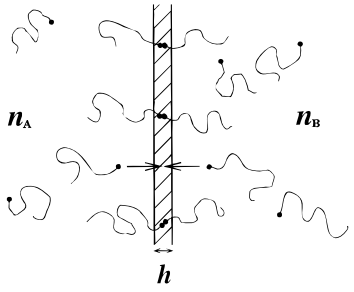

Figure 1. General situation studied in this paper. Two polymer melt bulks, separated by an interface of width h, contain reactive polymers at densities n_a and n_b. These bear functional end groups which can meet in the interface region only. Each reaction produces an AB diblock copolymer at the interface; as time progresses, the surface density of diblocks builds up and eventually reduces the interfacial reaction rate.

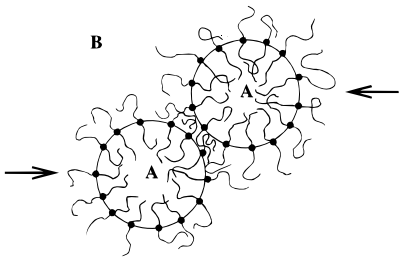

Figure 2. Reactive blending of two immiscible polymers A and B involves the formation of A−B diblocks at interfaces separating droplets from the continuous phase. The steric hindrance of diblock brushes at droplet surfaces appears to strongly reduce droplet coalescence rates. This leads to significantly smaller droplets in steady state.

[⊗] Abstract published in *Advance ACS Abstracts,* August 15, 1996.

S0024-9297(96)00117-9 CCC: $12.00

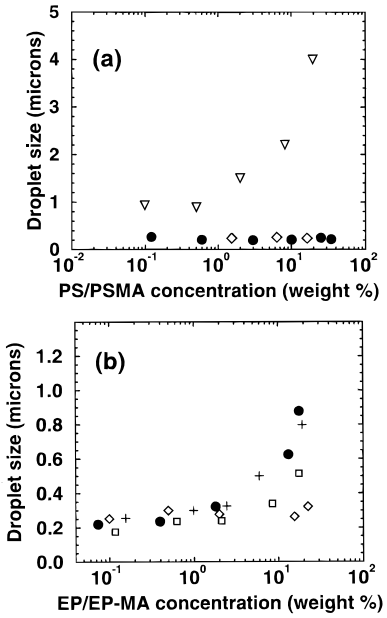

Figure 3. Reactive blending measurements by Sundararaj and Macosko:[7] number average droplet size as a function of dispersed phase concentration after blending at 200 °C for 12 min at a maximum shear rate of 65 s^{-1}. (a) Figure 10 of ref 7. Polystyrene−maleic anhydride (PSMA) of variable molecular weight and MA functionality, dispersed in polyamide-6,6 (diamino functional); (●) PSMA, mol wt 225k, 17 mol % MA; (◊) PSMA, mol wt 185k, 1.5% MA; (▽) 0% MA (nonreactive PS, mol wt 200k). MA groups, random along the PSMA backbone, can react with each of the two terminal amines of the polymamide-6,6. (b) Figure 8 of ref 7. Ethylene−propylene (EP) or ethylene−propylene−maleic anhydride (EP−MA), mol wt 84k, dispersed in polystyrene (PS) or polystyrene−oxazoline (PS−Ox), mol wt 200k, using various compatiblization methods: (●) PS/EP−MA (nonreactive system); (◊) PS−Ox/EP−MA (reactive groups random along backbone: 1% Ox react with 0.7% MA); (□) PS/EP with added diblock copolymer (Kraton G 37% styrene, mol wt 133k); (+) PS/EP with added triblock copolymer (Kraton G 32% styrene, mol wt 275k).

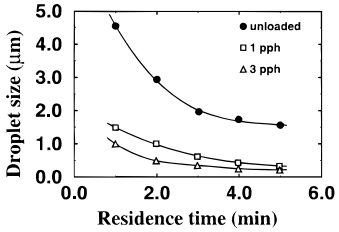

Figure 4. Droplet size as a function of residence time in a reactive processing extruder, for different concentrations (parts per hundred) of coupling agent (γ-aminopropyl)triethoxysilane (APS) (measurements by Okamoto and Inoue[6]). Both polymers are end functionalized: Carboxyl-terminated butadiene oligomer (mol wt 4800), 20% by wt, dispersed in hydroxy-terminated poly(ϵ-caprolactone) (mol wt 40k). All experiments performed at rotor speed 100 rpm at 120 °C.

It is the aim of this paper to answer these questions for the simplest model situation of this kind, depicted in Figure 1. Two bulk polymer melt phases A and B, separated by an interface of thickness h and area A, each contain a small fraction of end-functionalized chains. Reactions between A and B chains can occur in the interfacial region only, each reaction producing an AB diblock. The object we will focus on in this study is the rate constant k, naturally defined in terms of the reaction rate per unit area:

$$\frac{1}{A}\frac{dM}{dt} = k n_A n_B \qquad (1)$$

where M is the total number of A−B pairs which have reacted after time t and n_A and n_B are the number densities of reactive chains in each phase. For simplicity, we take A and B chains to have the same degree of polymerization N, and we will treat the experimentally relevant case where the root mean square (rms) coil size R is much greater than the interface thickness h. Typical values are[1,17,18] $R \approx 500$ Å and $h \approx 30$ Å.

As time progresses and the area per diblock $\Sigma \equiv A/M$ diminishes, so k will be reduced. However, we will begin our study by considering first the bare interface. In this case we will establish two limits depending on the magnitude of the local functional group reactivity, Q. We assume that the "capture radius" is of the same order as the reactive group size a. Thus Q is the reaction probability per unit time when a pair of A−B reactive groups are in contact. Now for the case of very small Q, correlations are only weakly perturbed from their equilibrium values and we will show that mean field theory is then applicable: k is proportional to the equilibrium contact probability between reactive groups.

The second and more complex case is large Q. To understand what happens in this diffusion-controlled limit, let us first briefly review polymer reaction kinetics in the *bulk*,[19] i.e. for situations where live chains can meet anywhere in the reaction vessel. Here the definition of k is slightly different, $\dot{n}_a = \dot{n}_b = -k n_a n_b$, implying that k has dimensions volume divided by time. The basic conclusion of theory[20−23] is that in melts the relevant scales characterizing k are the large polymer dimensions R and τ, the coil size, and relaxation time, respectively:

$$k \approx R^3/\tau \qquad \text{(bulk)} \qquad (2)$$

Since chemical reaction requires a group separation of a or less, one might naively have anticipated $k \approx a^3/t_a$ where t_a is the relaxation time of a single chain unit. This is incorrect because the small time scale monomer motion ($t < \tau$) guarantees that reaction occurs whenever the coil volumes of two reactive polymers overlap; in consequence the coil size R emerges as an *effective* capture radius. The reader is referred to refs 20−23 for more detailed discussions.

The essential point is that the large Q interfacial reaction problem is analogous to one in the bulk, but with the spatial dimension incremented by 1. This was shown for the case of small molecules in ref 14, and a similar logic applies here. The first hint at this fact comes from the dimensions of the interfacial k; from eq 1 these are length to the fourth power divided by time. Note that reaction requires the simultaneous arrival at the interface of two chains, one from either side. This is very different from the problem of irreversible polymer adsorption at a surface, which is in effect a one-dimensional reaction-diffusion problem. To establish the effective dimensionality in the present case, it is conceptually helpful to consider a general d-dimensional space (see Figure 5). Then $2d$ variables are needed to specify the locations of a pair of functional groups which can react with each other. Reaction is only possible if the groups are at the same point on the $d - 1$-dimensional interface; that is, there are $d - 1$ degrees of freedom associated with the reaction "sink." This leaves $2d - (d - 1) = d + 1$ extra degrees of freedom; we have, in effect, a $(d + 1)$-dimensional bulk reaction-diffusion problem. Noting that the generalization to arbitrary dimension of the result of eq 2 is $k \approx R^d/\tau$, and returning to three-dimensional space, it follows that

$$k \approx R^4/\tau \qquad \text{(interface)} \qquad (3)$$

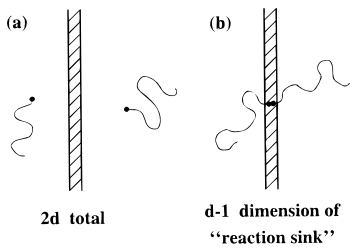

Figure 5. (a) For a general d-dimensional space, there are $2d$ degrees of freedom associated with the end groups of an A−B pair. (b) The generalized "reaction sink" has $d - 1$ dimensions. The difference between these two numbers, $d + 1$, is the effective dimensionality of the interface reaction-diffusion problem.

This result will be derived more rigorously in section III. For unentangled melts, where[1,24] $\tau \sim N^2$ (Rouse dynamics) it suggests that k is independent of N since statics are ideal, $R \sim N^{1/2}$. In fact, detailed calculation leads to a logarithmic correction to this expectation, $k \sim 1/\ln N$. Meanwhile in entangled melts, where[1,24] $\tau \sim N^3$ according to reptation theory, the prediction is $k \sim 1/N$. These molecular weight dependencies are very different from those predicted for bulk reactions:[20,21] $k \sim 1/N^{1/2}$ and $k \sim 1/N^{3/2}$ for unentangled and entangled melts, respectively.

In the following section a general result for the interfacial reaction rate constant k will be derived. As for bulk reactions,[20,21,23] the crucial component of this expression is the time integral of the return probability, $S(t)$. Essentially, this is the probability that a pair of A−B end groups, whose reactivity has been "switched off", are in contact with one another at time t given initial contact. Section III examines the structure of $S(t)$, and in sections IV and V these general results are applied to the specific situations of unentangled and entangled melts, respectively. In section VI we consider how the increase of diblock surface density reduces the area available for reaction and diminishes k; at high coverages, we find that k is exponentially small in diblock surface density. Section VII offers some general conclusions, including a brief discussion of the implications of these results for reactive processing.

II. General Result for Rate Constant *k*

A precise definition of the interface thickness h is obtained from the equilibrium pair distribution function, $P_{eq}(\mathbf{r}_a,\mathbf{r}_b)$, where $\mathbf{r}_a$ and $\mathbf{r}_b$ label the functional groups of a reactive A and B chain, respectively. Taking the x direction orthogonal to the interface, we choose that the A and B bulk phases occupy, respectively, $x < 0$ and $x > 0$ with the interface centered at $x = 0$. We define[25]

$$h \equiv \int \mathrm{d}x\, P_{eq}(\mathbf{r},\mathbf{r})/P_\infty \tag{4}$$

where P_∞ is the value of P_{eq} when both chains are far from the interface ($P_\infty = 1/(V_A V_B)$ where V_A and V_B are the volumes of the A and B bulks, respectively). For example, in the case of an infinitely sharp interface one has $P_{eq}(\mathbf{r}_a,\mathbf{r}_b) = P_\infty \Theta(h/2-x_a)\,\Theta(x_b+h/2)$ where $\Theta(x)$ is the step function.

Suppose reactions are "switched on" at $t = 0$. Then the time-dependent pair distribution function $P_t(\mathbf{r}_a,\mathbf{r}_b)$ approximately satisfies

$$P_t(\mathbf{r}_a,\mathbf{r}_b) = P_{eq}(\mathbf{r}_a,\mathbf{r}_b) - Qa^3 \int_0^t \mathrm{d}t' \int \mathrm{d}\mathbf{r}'\, G_{t-t'}(\mathbf{r}_a,\mathbf{r}_b;\mathbf{r}',\mathbf{r}')\, P_{t'}(\mathbf{r}',\mathbf{r}') \tag{5}$$

where the Green's function $G_t(\mathbf{r}_a,\mathbf{r}_b;\mathbf{r}'_a,\mathbf{r}'_b)$ is the probability density that (in the absence of reactions) the end groups of an A−B pair are at $\mathbf{r}_a$, $\mathbf{r}_b$ at time t given initial locations $\mathbf{r}'_a$, $\mathbf{r}'_b$. This self-consistent expression equates P_t to the value it would have had without reactions (P_{eq}), minus the number of pairs which reacted at previous times within $\mathrm{d}t'$ of t' (of which $Q\,\mathrm{d}t'\,a^3\,P_{t'}(\mathbf{r}',\mathbf{r}')$ per unit volume reacted at $\mathbf{r}'$) and subsequently arrived at $\mathbf{r}_a$, $\mathbf{r}_b$ at the time t, summed over all t' and $\mathbf{r}'$. The reader is referred to refs 21 and 23 for extensive discussions of this relationship.

It is important to note that eq 5 is an *approximation*, one which has been widely employed by theoreticians studying polymer reactions.[20,21,23,26] However, there is a great deal of evidence from near-exact renormalization group studies,[22,27,28] in which eq 5 is replaced by the exact relationship, that although this approximation leads to incorrect numerical coefficients in k, it does always generate the correct dependencies of k on molecular weight. This point is discussed in detail in ref 23. For the purposes of the present study, therefore, we can use the above framework to predict the functional dependencies of k on molecular weight and interface thickness with confidence. Since prefactors are unreliable, we will mainly ignore them in what follows.

As time proceeds, the normalization of P_t decreases, due to reactions, from its initial value of unity. Integrating eq 5 over all coordinates and using the normalization property of G_t, one obtains the following expression for the reaction rate per unit area (for the two-chain problem)

$$R \equiv -\frac{1}{A}\frac{\mathrm{d}}{\mathrm{d}t}\int \mathrm{d}\mathbf{r}_a\, \mathrm{d}\mathbf{r}_b\, P_t(\mathbf{r}_a,\mathbf{r}_b) = QP_t^{\mathrm{cont}} \tag{6}$$

where P_t^{cont} is the reactive group contact probability per unit area at time t,

$$P_t^{\mathrm{cont}} = a^3 \int \mathrm{d}x\, P_t(\mathbf{r},\mathbf{r}) \tag{7}$$

Here we have made use of an important feature of this problem: while translational invariance in the x direction is broken by the interface, it is retained in the transverse directions. Thus one may replace $\int \mathrm{d}\mathbf{r} \rightarrow A\int \mathrm{d}x$.

Now the total rate at which A−B pairs react is Rn_An_B/P_∞ per unit area, n_An_B/P_∞ being the total number of A−B chain pairs in the system. From its definition in eq 1, it follows that k and R are simply related as $k = R/P_\infty$. Using the definition of h, eq 4, we thus have

$$k = Qa^3 h \Pi_t^{\mathrm{cont}} \qquad \Pi_t^{\mathrm{cont}} \equiv P_t^{\mathrm{cont}}/P_{\mathrm{eq}}^{\mathrm{cont}} \tag{8}$$

where Π_t^{cont} is the dimensionless contact probability, measured relative to its initial equilibrium value $P_{\mathrm{eq}}^{\mathrm{cont}}$. Thus $\Pi_0^{\mathrm{cont}} = 1$.

It is now evident that we must first evaluate Π_t^{cont} if we wish to derive k. In Appendix A we show that Π_t^{cont} obeys the following dynamics:

$$\Pi_t^{\mathrm{cont}} = 1 - Qa^3 \int_0^t \mathrm{d}t'\, S(t-t')\Pi_{t'}^{\mathrm{cont}} \tag{9}$$

Here the return probability $S(t)$ is the probability that a reactive pair are in contact at time t given that they were initially in contact in the interfacial region:

$$S(t) = \int \mathrm{d}\mathbf{r}\, G_t(\mathbf{r},\mathbf{r};0,0) \tag{10}$$

Since contact outside this region is improbable, $S(t)$ is

essentially the probability that the pair are once again in contact in the interfacial region at time t.

Laplace transforming eq 9 and solving for Π in the large time limit, one obtains for the long time rate constant (see refs 21 and 23 for similar manipulations)

$$k = \frac{Qa^3h}{1 + Qa^3\int_0^\infty \mathrm{d}t\ S(t)} \tag{11}$$

This general result is very similar to that for bulk problems;[21,23] the important differences are the appearance of h and the structure of the return probability $S(t)$, which is fundamentally modified by the presence of the interface. As for bulk problems, k is determined by the time integral of S.

In the following section we will establish the general structure of $S(t)$. It is essential to observe that $S(t)$ and G_t refer to the dynamics of a pair of *nonreactive* end groups,[21,23] i.e. they describe end group behavior in the standard situation of an A−B polymer system in equilibrium. This stems from the basic dynamics of eq 5 whose usefulness is that it relates P_t (describing the reacting system) to P_{eq} and G_t (describing the nonreacting equilibrium system).

III. The Return Probability $S(t)$

Remembering that $R \gg h$, it is natural to anticipate that the dominant contribution to $\int_0^\infty S$ will derive from times much greater than t_h, the time for a chain end to diffuse a distance h. This will be demonstrated later (see Appendix C). For such times, it is argued in Appendix B that the structure of the Green's function determining S (eq 10) is as follows:

$$G_t(\mathbf{r}_a,\mathbf{r}_b;0,0) = \frac{1}{x_t^6}\frac{P_{eq}(\mathbf{r}_a,\mathbf{r}_b)}{P_\infty} F\left(\frac{x_a}{x_t},\frac{\mathbf{r}_{aT}}{x_t},\frac{x_b}{x_t},\frac{\mathbf{r}_{bT}}{x_t},\frac{x_t}{R}\right) \qquad (t \gg t_h) \tag{12}$$

where x_a and $\mathbf{r}_{aT}$ are the locations of group A in the orthogonal and transverse directions, respectively. Similarly, $\mathbf{r}_b \equiv (x_b, \mathbf{r}_{bT})$. G_t involves a product of the equilibrium distribution function P_{eq} with a dimensionless scaling function F whose important feature is its independence of $\mathbf{r}_a$ and $\mathbf{r}_b$ in the limit when r_a and r_b are much less than the rms displacement of a chain end after time t, namely x_t. That is, $F(u,\mathbf{v},w,\mathbf{z},\delta) \to \hat{F}(\delta)$ for $u, v, w, z \ll 1$, where $\hat{F}(\delta)$ has magnitude of order unity. We have assumed in eq 12 that x_t is identical for polymer types A and B. In Appendix B, a distinction is maintained between monomer displacements orthogonal and parallel to the interface, whereas in eq 12 this distinction has been dropped for simplicity. We expect this to be valid up to constant prefactors, i.e. the two quantities will scale with time in the same way. In any case, it is straightforward to drop this assumption; none of the essential conclusions which follow are modified.

The small argument property of F described above is crucial: it implies that G_t scales as the *equilibrium pair distribution function* P_{eq} on length scales less than x_t. This is physically reasonable; the region $r_a, r_b < x_t$ is that which, by the time t, has been explored by the two end groups. Assuming ergodic dynamics, relative probabilities should thus be as in equilibrium.[23,29] As shown in Appendix B, this is in fact a direct consequence of the principle of detailed balance.[23]

Inserting this expression for G_t into the definition of S, eq 10, one has

$$S(t) \approx \frac{1}{x_t^6}\int \mathrm{d}\mathbf{r}\ \frac{P_{eq}(\mathbf{r},\mathbf{r})}{P_\infty} F(0,\mathbf{r}_T/x_t,0,\mathbf{r}_T/x_t,x_t/R) \qquad (t \gg t_h) \tag{13}$$

where the x direction arguments of F have been set to zero. This is justified for these large values of $x_t \gg h$ because $P_{eq}(\mathbf{r},\mathbf{r})$, and hence the integrand itself, is substantial for $|x| \lesssim h$ only; the probability that both groups are well into the same bulk phase, either the A or the B one, is tiny. Integrating over x, we collect a factor h (recall our definition, eq 4) and the transverse integration then leads to the following general structure:

$$S(t) \approx \frac{h}{x_t^4} g(x_t/R) \qquad (t \gg t_h) \tag{14}$$

where g is another scaling function whose magnitude is always of order unity.

The above form should be compared with that for *bulk* reactions in the melt,[21] where $S \sim 1/x_t^3$ scales as the inverse of the volume explored by a reactive group after time t. This would generalize to $S \sim 1/x_t^d$ for a general d-dimensional bulk problem. In the presence of the interface, one sees that the return probability of eq 14 is reduced, relative to the bulk value, by the fraction of the volume explored which is occupied by the interface, namely h/x_t. In consequence, the time dependence of $S(t) \sim 1/x_t^4$ is that of a *four*-dimensional bulk reaction problem. This is in accordance with our general arguments of section I.

IV. Unentangled Melts

In the previous section a general form was established for the return probability, eq 14. Let us now specialize this result to the particular case of unentangled melts, where polymer dynamics are Rouse-like:[1,24] $R \sim N^{1/2}$ and $\tau \sim N^2$. Integrating $S(t)$ over time will give k via eq 11.

In this case x_t has the simple structure[24]

$$x_t = Rf(t/\tau) \qquad f(u) \approx \begin{cases} u^{1/4}, & u \ll 1 \\ u^{1/2}, & u \gg 1 \end{cases} \tag{15}$$

where the function f interpolates between the short time $t^{1/4}$ and long time Fickian $t^{1/2}$ regimes. From eq 14, the total contribution from times greater than t_h is

$$\int_{t_h}^\infty \mathrm{d}t\ S(t) \approx \frac{h\tau}{R^4}\int_{t_h/\tau}^\infty \mathrm{d}u\ \theta(u) \approx \frac{h\tau}{R^4}\ln(\tau/t_h)$$

$$\theta(u) \approx \begin{cases} 1/u, & u \ll 1 \\ 1/u^2, & u \gg 1 \end{cases} \tag{16}$$

where $\theta(u) \equiv g(f(u))/f^4(u)$. We have used the fact that both $g(0)$ and $g(\infty)$ are constants of order unity. The cutoff at t_h leads to a logarithmic factor $\ln \tau/t_h = 4 \ln R/h$. We show in Appendix C that contributions from the shortest times, $t < t_h$, lead to higher order terms. Returning to the general result for k, eq 11, one obtains

$$k = \frac{Qa^3h}{1 + Qt_a(h/a)\ln(R/h)} \tag{17}$$

This is our final result for unentangled melts, valid for any value of the local reactivity Q.

In the limit of weakly reactive groups, small Q, k describes mean field (MF) kinetics[23]

$$k = Qa^3h \qquad (Q \ll Q^*) \tag{18}$$

whereas diffusion-controlled (DC) kinetics are realized for large Q:

$$k = \frac{a^4}{t_a}\frac{1}{\ln(R/h)} \sim \frac{1}{\ln N} \qquad (Q \gg Q^*) \tag{19}$$

The MF/DC crossover occurs at a value

$$Q^* \equiv \frac{1}{t_a}\frac{a}{h\ln(R/h)} \tag{20}$$

In summary, for long unentangled chains and strongly reactive functional groups, k has weak logarithmic dependencies on chain length N and interface width h.

V. Entangled Melts

For sufficiently long chains, $N > N_e$ where N_e is the entanglement threshold,[1,24,30] chain mobility is strongly reduced by entanglements. Our framework here will be the reptation model,[1,24] according to which the motion of each polymer is confined to a tube of diameter $b = N_e^{1/2}a$ by the entangling environment composed of other chains. We will assume here that $h \ll b$.

In Appendix D we show that the time integral of S has a form very similar to that for the unentangled case (eq 16) but with $\tau \approx (N^3/N_e)t_a$ now representing the reptation time[1,24] rather than the Rouse time:

$$\int_0^\infty \mathrm{d}t\ S(t) \approx \frac{h\tau}{R^4}\ln(\tau/T_N) \tag{21}$$

Note also that the logarithm now involves the "breathing time"[24] $T_N = N^2t_a$ (see Appendix D) instead of t_h. Thus one obtains

$$k = \frac{Qa^3h}{1 + Qt_a(h/a)(N/N_e)\ln(N/N_e)} \tag{22}$$

For small values of the local reaction rate Q, this leads to the same MF limit as for unentangled systems, eq 18. For strongly reactive groups, the DC limit is now

$$k = \frac{a^4}{t_a}\frac{1}{(N/N_e)\ln(N/N_e)} \sim \frac{1}{N\ln N} \qquad (Q \gg Q^*) \tag{23}$$

Comparing with the unentangled case of the previous section, the dependencies on chain length are now much stronger both for k and for the threshold for DC behavior which is now at a value

$$Q^* \equiv \frac{1/t_a}{(h/a)(N/N_e)\ln(N/N_e)} \tag{24}$$

VI. Excluded Area Effects at the Interface

Thus far we have treated a bare interface. As the area Σ per chain of diblock product decreases, so the interface becomes increasingly inaccessible to reactive free chains from the A and B bulks. At sufficiently high surface density, the diblock brush formed at the A−B interface becomes extended relative to the unperturbed coil size $R = N^{1/2}a$; when this happens, one expects that the density of mobile bulk chains near the interface will drop significantly below the bulk values n_a and n_b with consequent reduction in k (see Figure 6).

Now the density profile of free bulk chains within a stretched brush has been addressed theoretically by de Gennes[31] and by Zhulina and Borisov,[32,33] who considered a melt in contact with a brush grafted to a solid surface. Zhulina and Borisov found that the brush is strongly stretched when Σ/a^2 drops below $N^{1/2}$, in which case the density profile within the brush is $\rho(x) = \rho_{bulk}\exp[Cx^2 - D(Na^3/\Sigma)^2]/Na^2$ where ρ_{bulk} is the bulk density and C and D are constants of order unity. Thus the density at the surface is exponentially small, $\rho(0) = \rho_{bulk}e^{-DNa^4/\Sigma^2}$. By contrast, for low coverages, $\Sigma/a^2 > N^{1/2}$, the density of free chains within the brush is essentially equal to its value far into the bulk, ρ_{bulk}.

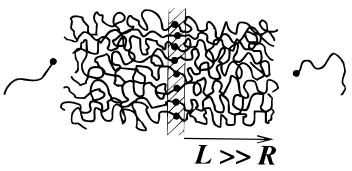

Figure 6. Reaction rates are exponentially suppressed when the interface becomes crowded with diblock product at values of the area per chain, Σ, which are less than $N^{1/2}a^2$. This corresponds to the diblock brush being stretched, i.e. its size L being much bigger than the unperturbed chain dimension R.

From the above, it is clear that provided $\Sigma/a^2 > N^{1/2}$, then the expressions for k we have obtained for the bare interface will remain valid. For the remainder of this section we ask what happens in the high-coverage case, when $\Sigma/a^2 < N^{1/2}$ and the brush is *strongly stretched*; that is, the extension of the brush, L, becomes large compared to R (see Figure 6). In our general expression for k, eq 11, we will see that by far the most important influence of the stretched brush is to render h, which features in the numerator, exponentially small. This is because h (see its definition, eq 4) is closely related to the equilibrium contact probability for an A−B pair; this probability becomes exponentially suppressed when both chains must penetrate the stretched brush before they can meet.

Let us begin, then, by determining h for this high-coverage situation. Suppose that the brush of area A consists of M_{brush}^{perm} A−B diblocks, that the A bulk contains $M_A = n_AV_A$ reactive chains and M_A' unreactive chains, and that the B bulk contains M_B reactive and M_B' unreactive chains. Let us now "switch off" reactions and consider M_{brush}^{temp}, defined to be the average number of "reactive" A−B homopolymer pairs whose functionalized ends are in contact with one another in equilibrium. Note that these pairs constitute M_{brush}^{temp} temporary extra diblocks in the brush, in addition to the M_{brush}^{perm} permanent members. Now M_{brush}^{temp} is directly related to $P_{eq}(\mathbf{r},\mathbf{r})$, being equal to the total contact probability for one end-functionalized A−B pair multiplied by the total number of end-functionalized pairs in the system, namely n_An_B/P_∞:

$$M_{brush}^{temp} = \int \mathrm{d}^3r\ a^3P_{eq}(\mathbf{r},\mathbf{r})\ n_An_B/P_\infty \tag{25}$$

whence

$$a^3h = \frac{M_{brush}^{temp}}{A}\frac{1}{n_An_B} \tag{26}$$

after using the definition of h, eq 4. Thus we now proceed to calculate M_{brush}^{temp}, which will immediately yield h via eq 26.

Now the weighting for a given value of M_{brush}^{temp} is the brush free energy $F_{AB}^{brush}(M_{brush}^{temp},M_{brush}^{perm})$ given that the brush contains M_{brush}^{temp} diblocks of one type, and M_{brush}^{perm} of another distinguishable but otherwise identical type. This free energy is calculated in Appendix E, following

the calculation of Semenov in ref 34, eq E5. It implies the following expression for the chemical potential of the temporary diblocks:

$$\frac{\mu_{\text{brush}}^{\text{temp}}}{T} = \frac{\partial F_{\text{AB}}^{\text{brush}}}{\partial M_{\text{brush}}^{\text{temp}}} = \ln \frac{M_{\text{brush}}^{\text{temp}} a^3}{A h_0} + 9\frac{L^2}{R^2} + 2(N-1)\ln\frac{e}{z-1} + 2\ln\frac{R}{L} + \text{const} \quad (27)$$

where $h_0 = a/(6\chi)^{1/2}$ is the bare interface thickness in the Helfand and Tagami theory[18] and χ is the Flory parameter. Note that the partial derivative with respect to $M_{\text{brush}}^{\text{temp}}$ is taken at constant $M_{\text{brush}}^{\text{perm}}$ and A, and that $LA = (M_{\text{brush}}^{\text{temp}} + M_{\text{brush}}^{\text{perm}})Na^3$ has been used.

Meanwhile the reactive chains in each bulk exert their chemical potentials upon each side of the brush. That of the *A* bulk is obtained from the result of eq F2 in Appendix F for the partition function, Z_{bulk}, of a bulk melt consisting of two distinguishable but otherwise identical chain types:

$$\frac{\mu_{\text{A}}}{T} = \frac{\partial}{\partial M_{\text{A}}} \ln Z_{\text{bulk}}(M_{\text{A}}, M'_{\text{A}}) = \ln n_{\text{A}} + (N-1)\ln\frac{e}{z-1} \quad (28)$$

where the derivative was taken at constant M'_{A} and we have used $V_{\text{A}} = (M_{\text{A}} + M'_{\text{A}})Na^3$. A similar expression follows for μ_{B}.

Now the condition for equilibrium (which determines $M_{\text{brush}}^{\text{temp}}$, given M_{A} and M_{B}) is that appropriate for the reversible diblock-forming "reaction" $A + B \rightleftharpoons$ diblock. That is,

$$\mu_{\text{A}} + \mu_{\text{B}} = \mu_{\text{brush}}^{\text{temp}} \quad (29)$$

Using our expressions for the three chemical potentials in eq 29, we solve eq 29 for $M_{\text{brush}}^{\text{temp}}$, which leads to the following expression for h from eq 26:

$$a^3 h = a^3 h_0 \frac{Na^4}{\Sigma^2} \exp(-9Na^4/\Sigma^2) \quad (30)$$

As anticipated, h is exponentially reduced by high coverage relative to its bare interface value, h_0. This drastically lowers k through eq 11.

What remains is to estimate the form of the return probability $S(t)$ appearing in eq 11. Now, roughly speaking, the configurational statistics of a diblock belonging to the brush are those of a chain which is uniformly stretched in the x direction on sufficiently large scales: $\Delta x \approx (L/N)\,\Delta n$. For smaller scales, $\Delta x < x_{\text{blob}}$, stretching effects are weak and random walk statistics are recovered: $\Delta x \approx a(\Delta n)^{1/2}$. The "blob" size, x_{blob}, is determined by equating these two laws:

$$x_{\text{blob}} = Na^2/L = \Sigma/a \quad (31)$$

Thus the portion of the brush within a distance x_{blob} of the A−B interface is unstretched. Now imagine suddenly cutting the diblock at its joint at time $t = 0$. This creates two pieces, the A block and the B block, each with a new free end. $S(t)$ is the probability density that at time t these two newly created ends happen to be together once again.

Consider firstly the motion of the new A end. Initially, it lies close to $x = 0$ ($|x| \lesssim h_0$) but since the A chain to which it is attached is strongly stretched, it will quickly be pulled away. Assuming this is an unentangled system, the problem amounts to an initially and uniformly stretched half-infinite Rouse chain with a stress free end. After time t, the free end boundary condition has had time to influence the first $n(t) \approx (t/t_{\text{a}})^{1/2}$ monomers of the A chain: this portion has had time to relax back to random walk statistics as in the unstretched state. Essentially, the distance x_t of the end from the A−B interface (of thickness h_0) is then determined by the statics on a scale of $n(t)$ monomers. That is, $x_t \approx a\{n(t)\}^{1/2}$ for $t < t_{\text{blob}}$, and $x_t \approx (L/N)\,n(t) = x_{\text{blob}}(t/t_{\text{blob}})^{1/2}$ for $t > t_{\text{blob}}$. Here $t_{\text{blob}} \equiv t_{\text{a}}(x_{\text{blob}}/a)^4$ is the Rouse time[24] for one blob; it separates short time dynamics which are of standard Rouse form, unmodified by the brush, from long time behavior which is dominated by the pull of the stretched chain. Note that since $t_{\text{blob}} > t_{h_0}$ (always true provided the chain is not completely stretched, $L = Na$) we have ignored the very shortest $t < t_{h_0}$ behavior which gives the same higher order contribution as for the bare interface (see Appendix C).

Now we can assemble $S(t)$ as follows. From the above remarks, for $t < t_{\text{blob}}$ the dynamics of both the A and the B end are as for the bare interface and $S(t) \approx h_0/x_t^4$ as before (see eq 14). This is conveniently rewritten $S(t) = (h_0/x_{\text{blob}}^4)(t_{\text{blob}}/t)$. The expression for $t > t_{\text{blob}}$ is quite different:

$$a^3 S(t) \approx \frac{h_0}{x_t^{\text{Rouse}}} f(x_t/x_t^{\text{Rouse}}) \times \frac{a}{x_t^{\text{Rouse}}} f(x_t/x_t^{\text{Rouse}}) \times \left(\frac{a}{x_t^{\text{Rouse}}}\right)^2 \quad (t > t_{\text{blob}}) \quad (32)$$

Here $x_t^{\text{Rouse}} = a\{n(t)\}^{1/2}$ is the standard Rouse dynamics displacement, and $f[(x_t - x_{\text{A}}^{\text{end}})/x_t^{\text{Rouse}}]$ is the probability distribution for $x_{\text{A}}^{\text{end}}$, namely the location of the A end in the x direction. This distribution is centered at $x_{\text{A}}^{\text{end}} = x_t$ and has width x_t^{Rouse}, this being the fluctuation in the end position. For $t > t_{\text{blob}}$, the interface at $x_{\text{A}}^{\text{end}} = 0$ is far off in the tail of the distribution, since $x_t/x_t^{\text{Rouse}} \gg 1$, and the end is very unlikely to be there; we expect that $f(u)$ becomes exponentially small for $u \gg 1$. The first and second factors in eq 32 are respectively the probability the A end lies within the interface and the probability the B end is within a distance a of the A end in the x direction. The third factor is the probability the B end is within a of the A end in the direction parallel to the interface (the lateral distribution of end locations also has width x_t^{Rouse}.)

Thus we may write

$$S(t) \approx \frac{h_0}{x_{\text{blob}}^4} g(t/t_{\text{blob}}) \quad g(u) = \begin{cases} 1/u, & u \ll 1 \\ f^2(u^{1/4})/u, & u \gg 1 \end{cases} \quad (33)$$

where we have rewritten $(1/x_t^{\text{Rouse}})^4 = (1/x_{\text{blob}})^4(t_{\text{blob}}/t)$ and $x_t/x_t^{\text{Rouse}} = (t/t_{\text{blob}})^{1/4}$. The important feature of g is that for large arguments it is very strongly cut off; *the return probability is negligible for times greater than* t_{blob}. Physically, the stretched chains have irretrievably pulled the ends well into their respective brushes for such times.

From eq 33 the dominant contribution to the time integral of S is thus

$$\int_{t_{h_0}}^{\infty} \mathrm{d}t\ S \approx \frac{h_0 t_{\mathrm{blob}}}{x_{\mathrm{blob}}{}^4} \int_{t_{h_0}/t_{\mathrm{blob}}}^{\infty} \mathrm{d}u\ g(u) \approx \frac{h_0 t_{\mathrm{a}}}{a^4} \ln[x_{\mathrm{blob}}/h_0] \tag{34}$$

which is the same as the corresponding expression for the bare interface, eq 16, except that $\tau \rightarrow t_{\mathrm{blob}}$ (or, equivalently, $R \rightarrow x_{\mathrm{blob}}$). We remark that even though a real brush has nonuniform stretch,[35] our uniformity assumption here correctly reproduces the essential feature of a sharp cutoff in $S(t)$ after t_{blob}. The errors introduced are unimportant since the stretch varies little over the length scales of interest here, $x \approx x_{\mathrm{blob}}$.

For entangled systems, let us assume that the blob size is less than the tube diameter, $t_{\mathrm{blob}} < t_b$. In this case eq 34 will follow once again, since reptation dynamics will then anyway be Rousian on time scales less than the cutoff scale t_{blob}.

Using eqs 34, 31, and 30 in eq 11, we obtain our final result for the rate constant at crowded interfaces:

$$k = \frac{Q\mathrm{a}^3 h_0 (Na^4/\Sigma^2) \exp(-9Na^4/\Sigma^2)}{1 + Qt_{\mathrm{a}}(h_0/a) \ln(\Sigma/ah_0)} \qquad (\Sigma < N^{1/2}a^2) \tag{35}$$

For small Q this gives the MF result

$$k = Qa^3 h_0 (Na^4/\Sigma^2) \exp(-9Na^4/\Sigma^2) \qquad (Q < Q^*) \tag{36}$$

while the large Q DC result reads

$$k = \frac{(a^4/t_{\mathrm{a}})(Na^4/\Sigma^2)}{\ln(\Sigma/ah_0)} \exp(-9Na^4/\Sigma^2) \qquad (Q > Q^*) \tag{37}$$

The crossover reactivity is now $Q^* = t_{\mathrm{a}}{}^{-1}a/[h_0 \ln(\Sigma/ah_0)]$.

By far the dominant factor in these expressions for k is the exponential one.[37] The principal conclusion of this section is that for the crowded interface $k \sim \exp(-9Na^4/\Sigma^2)$.

VII. Conclusions

For weakly reactive functional groups, we have seen that reaction kinetics obey mean field theory: $k = Qa^3h$. That is, k is proportional to the total contact probability per unit area in *equilibrium*, namely $\int_{-\infty}^{\infty} \mathrm{d}x\ a^3\ P_{\mathrm{eq}}(\mathbf{r},\mathbf{r})$. From eq 4, this is just a^3h, to within a constant prefactor. As an example, consider the theory of Helfand and Tagami[17,18] where the density of A varies as $\rho_{\mathrm{a}}(x)/\rho(\infty) = \{1 + \exp[C\chi^{1/2}x/a]\}^{-1}$ where C is a positive constant of order unity. The density of B is determined by incompressibility, $\rho_{\mathrm{a}} + \rho_{\mathrm{b}} = \rho(\infty)$. Theirs is a mean field theory in which fluctuations are neglected, so $P_{\mathrm{eq}}(\mathbf{r}_{\mathrm{a}},\mathbf{r}_{\mathrm{b}})/P_\infty = \rho_{\mathrm{a}}(x_{\mathrm{a}})\rho_{\mathrm{b}}(x_{\mathrm{b}})/\rho^2(\infty)$. Inserting this approximate form for the pair distribution function into the formula for h of eq 4, one finds $h = C'a/\chi^{1/2}$ where C' is another constant of order unity. To within a multiplicative constant, this is the same as the expression for the interface thickness derived in ref 18. In this case, therefore, the weakly reactive limit reads $k \approx Qa^4/\chi^{1/2}$.

When the functional groups are sufficiently reactive, the kinetics become diffusion-controlled (DC). The calculations of sections IV and V have confirmed our general arguments of the Introduction, indicating also small logarithmic corrections. The DC result of eq 19 for unentangled systems can be written

$$k \approx \frac{R^4}{\tau} \frac{1}{\ln(\tau/t_h)} \sim \frac{1}{\ln N} \qquad \text{(unentangled, DC limit)} \tag{38}$$

The dependence on both molecular weight and interface thickness is logarithmic.

For entangled systems (eq 23) one has a much stronger molecular weight dependence, while the dependence on h disappears completely:

$$k \approx \frac{R^4}{\tau} \frac{1}{\ln(\tau/T_N)} \sim \frac{1}{N \ln N} \qquad \text{(entangled, DC limit)} \tag{39}$$

An interesting feature is that the threshold for DC kinetics, as in the case of bulk reactions,[23] is itself dependent on molecular weight. For the case of entangled melts, the dependence of the threshold value of the local reactivity is strong: $Q^* \sim 1/(N \ln N)$ (eq 24). Thus, the longer the reacting chains the less reactive the functional groups need be for the DC limit to be realized. Considering typical values $h/a \approx 5$ and $N/N_{\mathrm{e}} \approx 10$, one finds $Qt_{\mathrm{a}} \approx 1/100$ is required for DC behavior. This is 2 orders of magnitude less reactive than what would be required to attain the small molecule DC limit, $Qt_{\mathrm{a}} \approx 1$.

Finally, we have found that crowding of the interface suppresses k to exponentially small values as soon as the area per chain drops below a critical value $\Sigma = \Sigma_{\mathrm{crit}} \sim N^{1/2}$:

$$k \sim \mathrm{e}^{-\mathrm{const}(\Sigma_{\mathrm{crit}}/\Sigma)^2} \quad (\Sigma < \Sigma_{\mathrm{crit}} \equiv a^2N^{1/2}) \tag{40}$$

That is, reactions are essentially *switched off* as soon as this critical coverage is reached. But Leibler[12] has shown that the reduction in surface tension γ due to the presence of interfacial diblocks at a polymer−polymer interface of this type is given by $-\Delta\gamma/kT \approx (a^2N^{1/3}/\Sigma)^3$ (this result is valid when the diblock coverage is high enough to form a dry brush). Thus the coverage at which the lateral diblock surface pressure first becomes large enough to substantially influence surface tension is $\Sigma \approx \Sigma_{\mathrm{st}} \equiv N^{1/3}a^2$. Hence at the critical coverage Σ_{crit} surface tension reductions are tiny, $-\Delta\gamma \sim 1/N^{1/2}$. Our conclusion, therefore, is that in reactive blending systems reactions are unable to produce significant reductions in surface tension. Before the reactions can position sufficient diblocks at the interface to substantially diminish surface tension, the reaction rates have become exponentially suppressed by crowding.

The essential point is that the bare surface tension is of the order of kT/a^2; a significant reduction in surface tension requires a free energy excess per unit area, due to the brush, of the same order. Thus the threshold value for the free energy per chain, F_{chain}, is $F_{\mathrm{chain}} \approx kT\ \Sigma/a^2$. On the other hand, the threshold value at which reactions first experience difficulty placing new diblocks at the interface is only $F_{\mathrm{chain}} \approx kT$. Since F_{chain} is a monotonic decreasing function of Σ, it follows that the surface tension threshold, Σ_{st}, must be less than the reaction suppression threshold, Σ_{crit}: in practice, Σ_{st} can never be attained through reactions. To quantify this argument, one notes that a high coverages the dominant contribution to the Σ-dependent part of the free energy per chain is the stretch term, $F_{\mathrm{chain}} \approx kT\ N/(\Sigma/a^2)^2$ (see eq E4). Equating F_{chain} to kT yields $\Sigma_{\mathrm{crit}} \sim N^{1/2}$; equating F_{chain} to $kT\ \Sigma/a^2$ yields $\Sigma_{\mathrm{st}} \sim N^{1/3}$.

The above observation implies that the principal role of reactions will be to generate copolymers such as to sterically hinder droplet−droplet coalescence. This is consistent with the measurements and interpretations of Sundararaj and Macosko,[7] whose data are shown in Figure 3. Even though at higher dispersed phase concentrations the uncompatibilized samples of Figure 3a exhibit an increased steady state droplet size, nonetheless the reactivity compatibilized samples attain the *same* droplet size independent of concentration. This strongly suggests that coalescence has been almost entirely eliminated in the reactive systems, because coalescence rates would otherwise show increases with increasing droplet volume fraction. (Indeed, this is presumably the origin of the higher droplet sizes in the more concentrated uncompatibilized samples.) The compatibilized droplets appear to be so small that their steady state dimensions become determined by "single droplet" physics and hence are independent of concentration. However, the data of Figure 3a do not preclude possible reductions in surface tension as well, since effects of compatibilization are apparent even at the lowest concentrations studied. This is in contrast to Figure 3b where the measured steady state droplet sizes for, respectively, uncompatibilized and reactively compatibilized systems converge at the lowest concentrations. At these concentrations coalescence effects are presumably negligible. This would suggest that the only influence of compatibilization is via reduced coalescence rates; although reactions deliver copolymers to the interface more efficiently than through simple physical addition, they cannot generate sufficient material to significantly diminish surface tension.

Turning now to the data of Okamoto and Inoue shown in Figure 4, the three curves can be thought of as corresponding to three different values of the local reactivity, Q, for otherwise identical systems. Apparently, the larger the Q value, the more copolymer product that has been generated at the interface at a given moment in time. This suggests mean field (MF) kinetics (eq 18). Were diffusion-control to pertain, Q dependence would be predicted to disappear (see eqs 19 and 23). These data also suggest that the ultimate steady state droplet size may possibly be independent of Q, i.e. that the reactions reach a saturation point. However, observations at later times would certainly be necessary to confirm this suspicion.

Acknowledgment. This work was supported by the National Science Foundation under grant no. DMR-9403566. We thank Oleg Bychuk for many stimulating discussions.

Appendix A. Dynamics of Dimensionless Contact Probability Π_t^{cont}

In this appendix we derive the dynamics of eq 9 obeyed by Π_t^{cont}.

Setting $\mathbf{r}_a = \mathbf{r}_b = \mathbf{r}$ in eq 5 and integrating, one has

$$\int d\mathbf{r}\, P_t(\mathbf{r},\mathbf{r}) = \int d\mathbf{r}\, P_{eq}(\mathbf{r},\mathbf{r}) - Qa^3 \int_0^t dt' \int d\mathbf{r}\, d\mathbf{r}'\, G_{t-t'}(\mathbf{r},\mathbf{r};\mathbf{r}',\mathbf{r}')\, P_{t'}(\mathbf{r}',\mathbf{r}') \quad \text{(A1)}$$

Now consider times $t \gg t_h$. Then since $P_{t'}(\mathbf{r}',\mathbf{r}')$ is substantial for $|x|' \lesssim h$ only (where $\mathbf{r}' \equiv (x', \mathbf{r}'_T)$) one can set $x' = 0$ in the last two arguments of $G_{t-t'}$ with small error. That is, changes in x' of order h have little effect on $G_{t-t'}$ for times much larger than t_h. Recalling that the interface does not upset translational invariance in the transverse directions, we can thus make this replacement

$$G_{t-t'}(\mathbf{r},\mathbf{r};\mathbf{r}',\mathbf{r}') \to G_{t-t'}(x,\mathbf{r}_T-\mathbf{r}'_T,x,\mathbf{r}_T-\mathbf{r}'_T;0,0) \quad \text{(A2)}$$

Hence eq A1 becomes

$$\int d\mathbf{r}\, P_t(\mathbf{r},\mathbf{r}) = \int d\mathbf{r}\, P_{eq}(\mathbf{r},\mathbf{r}) - Qa^3 \int_0^t dt' \int d\mathbf{r}\, G_{t-t'}(\mathbf{r},\mathbf{r};0,0) \int d\mathbf{r}'\, P_{t'}(\mathbf{r}',\mathbf{r}') \quad \text{(A3)}$$

At this point we note that for $t \ll t_h$ one reovers (see Appendix D) a bulklike situation; i.e., the interface is itself like a bulk, its finite width contributing a small surface effect. The translational invariance is approximately recovered for all coordinates; i.e. one may replace $G_{t-t'}(\mathbf{r},\mathbf{r};\mathbf{r}',\mathbf{r}') \to G_{t-t'}(\mathbf{r}-\mathbf{r}',\mathbf{r}-\mathbf{r}';0,0)$ in eq A1, and eq A3 follows once again. The conclusion is that this result is true for *all* times other than a small region around $t = t_h$.

Dividing all terms in eq A3 by $\int d\mathbf{r}\, P_{eq}(\mathbf{r},\mathbf{r})$, one obtains eq 9 in the main text.

Appendix B. Scaling Form of Green's Function $G_t(\mathbf{r}_a,\mathbf{r}_b;0,0)$

In this appendix we will derive the scaling form for G_t of eq 12, as appropriate to a bare interface. The principle of detailed balance dictates that in the equilibrium state the transition rate from $(\mathbf{r}'_a, \mathbf{r}'_b)$ to $(\mathbf{r}_a, \mathbf{r}_b)$ equals that in the reverse direction:

$$G_t(\mathbf{r}_a,\mathbf{r}_b,\mathbf{r}'_a,\mathbf{r}'_b)\, P_{eq}(\mathbf{r}'_a,\mathbf{r}'_b) = G_t(\mathbf{r}'_a,\mathbf{r}'_b,\mathbf{r}_a,\mathbf{r}_b)\, P_{eq}(\mathbf{r}_a,\mathbf{r}_b) \quad \text{(B1)}$$

Now consider $r'_a, r'_b \ll x_t$. Then the $\mathbf{r}'_a$ and $\mathbf{r}'_b$ arguments in G on the left hand side of eq B1 may be set to zero with small error. This is the principle of finite memory: the initial conditions $\mathbf{r}'_a$, $\mathbf{r}'_b$ will be forgotten after a time scale much greater than the diffusion time corresponding to $\mathbf{r}'_a$, $\mathbf{r}'_b$. That is, when the width of G as a function of $\mathbf{r}_a$, $\mathbf{r}_b$ greatly exceeds the magnitude of $\mathbf{r}'_a$ and $\mathbf{r}'_b$, then one may simply replace these coordinates with zero. Now if we also choose $r_a, r_b \ll x_t$, we may similarly set the $\mathbf{r}_a$, $\mathbf{r}_b$ variables in G on the right hand side of eq B1 to zero. It follows that

$$G_t(\mathbf{r}_a,\mathbf{r}_b,0,0)/G_t(\mathbf{r}'_a,\mathbf{r}'_b,0,0) \approx P_{eq}(\mathbf{r}_a,\mathbf{r}_b)/P_{eq}(\mathbf{r}'_a,\mathbf{r}'_b) \quad \text{(B2)}$$

provided all four variables have magnitudes much less than x_t. We conclude that $G_t(\mathbf{r}_a,\mathbf{r}_b,0,0)$ is proportional to $P_{eq}(\mathbf{r}_a,\mathbf{r}_b)$ in this limit. This argument is very similar to that in ref 23 in the context of bulk polymer reactions.

This result motivates the following scaling ansatz on G_t:

$$G_t(\mathbf{r}_a,\mathbf{r}_b;0,0) = A_t \frac{P_{eq}(\mathbf{r}_a,\mathbf{r}_b)}{P_\infty} \tilde{F}\left(\frac{x_a}{x_t},\frac{\mathbf{r}_{aT}}{x_{tT}},\frac{x_b}{x_t},\frac{\mathbf{r}_{bT}}{x_{tT}},\frac{x_t}{R},\frac{x_{tT}}{R}\right) \quad (t \gg t_h) \quad \text{(B3)}$$

where x_{tT} is the rms displacement in the transverse direction after time t. We have assumed that the only scales in G_t are the displacements x_t and x_{tT} and the coil size R. In fact, for $t \lesssim t_h$ other scales such as h will enter, generating extra arguments such as x_t/h. For convenience we have considered $t \gg t_h$ above; these arguments are then small and drop out. The prefactor A_t depends on time only and is determined by the normalization of G_t.

The function $\tilde{F}$ of eq B3 has two essential asymptotic properties: (1) for large values of its scaled $\mathbf{r}_a$, $\mathbf{r}_b$ variables it decays rapidly to zero; (2) for small values of these variables, from the result of eq B2 $\tilde{F}$ must become *independent* of these variables.

Since we expect that x_t, x_{tT} will scale with time in the same manner, for the remainder of this appendix and in the main text we will cease to distinguish between them. Setting $x_t = x_{tT}$ in eq B3, we then integrate over all $\mathbf{r}_a$, $\mathbf{r}_b$ values and note that for almost all of this domain of integration one may replace $P_{eq}(\mathbf{r}_a,\mathbf{r}_b) \rightarrow P_\infty$ (since $x_t \gg h$). This leads to $A_t = (1/x_t^6)H(x_t/R)$ where H is another scaling function, giving the result of eq 12 in which $F \equiv H\tilde{F}$.

Appendix C. Corrections to $\int_0^\infty S$ from $t < t_h$

For small times, $t < t_h$, the form of $S(t)$ is as in the bulk; the A−B chain ends which are together at time $t = 0$ do not "know" about the finite size of the interface. Thus[21] $S \sim 1/x_t^3$. Using eq 15, it follows that the small time contribution to the time integral of S in the case of unentangled melts (Rouse dynamics) is

$$\int_0^{t_h} \mathrm{d}t\ S \approx (\tau/R^3)\int_0^{t_h/\tau} \mathrm{d}u/u^{3/4} \approx h\tau/R^4 \qquad \text{(Rouse)} \tag{C1}$$

This is small (albeit only logarithmically so) relative to the contribution from times $t > t_h$ exhibited in eq 16.

Turning now to entangled regimes, for $t < t_h$ the reptation dynamics[24] are Rouse-like since the tube diameter b has been assumed much greater than h. Thus $x_t = b(t/t_b)^{1/4}$ where t_b is the entanglement time, $t_b \equiv N_e^2 t_a$. Noting that $t_h/t_b = (h/b)^4$, one finds

$$\int_0^{t_h} \mathrm{d}t\ S \approx ht_b/b^4 \qquad \text{(reptation)} \tag{C2}$$

Since $t_b/b^4 = (N_e/N)\tau/R^4$, this is a small correction to the expression of eq 21.

Appendix D. Time Integral of Return Probability for Entangled Melts

For times less than the entanglement time $t_b \equiv N_e^2 t_a$, reptation dynamics[24] are Rouse-like: $x_t = b(t/t_b)^{1/4}$. During the regime $t_b < t < T_N$, where $T_N \equiv (N/N_e)^2 t_b$ is the Rouse time for the one-dimensional tube motion, one has $x_t = b(t/t_b)^{1/8}$; these are the "breathing modes". For longer times

$$x_t = R\tilde{f}(t/\tau) \qquad (t > T_N) \tag{D1}$$

where $\tilde{f}(u \ll 1) \approx u^{1/4}$ and $\tilde{f}(u \gg 1) \approx u^{1/2}$. The scaling function $\tilde{f}$ is similar to f describing Rouse dynamics (see eq 15). Using our general result for $S(t)$ of eq 14 and recalling that $t_h \ll t_b$ has been assumed, we obtain

$$\int_{t_h}^\infty \mathrm{d}t\ S(t) \approx \frac{h}{b^4}\int_{t_h}^{t_b} \mathrm{d}t\ \frac{t_b}{t} + \frac{h}{b^4}\int_{t_b}^{T_N} \mathrm{d}t\ \left(\frac{t_b}{t}\right)^{1/2} + \frac{h}{R^4}\int_{T_N}^\infty \mathrm{d}t\ \tilde{\theta}(t/\tau) \tag{D2}$$

where $\tilde{\theta} \equiv g(\tilde{f}(u))/\tilde{f}^4(u)$ is the analogous function to $\theta(u)$ in the unentangled case. Similarly to that case, the last integral in eq D2 gives $(h\tau/R^4)\ln(\tau/T_N)$. The first two integrals give contributions of order $(ht_b/b^4)\ln t_b/t_h$ and $(ht_b/b^4)(T_N/t_b)^{1/2}$, respectively. Observing that $(T_N/t_b)^{1/2} = (N/N_e)$ and that $\tau/R^4 = (t_b/b^4)(N/N_e)$, it follows that the last of these three integrals provides the dominant contribution. Since the $t < t_h$ part is shown in Appendix C to be of higher order, this third integral is in fact to leading order the complete time integral of $S(t)$. This is the result of eq 21.

Appendix E. Free Energy of Diblock Brush at A−B Interface

Consider a brush comprising M_{brush} A−B diblocks at the interface of our two immiscible bulk melts A and B. Each bulk chain is of length N; each diblock, of length $2N$. We assume the brush is stretched and therefore dry[31] (i.e., devoid of bulk chains).

Following Semenov[34] we "construct" the brush, starting from a grafted half A brush and a grafted half B brush each of height L and are A. The partition function of the A brush, consisting of M_{brush} A chains each of which has one end grafted (fixed) near but away from the A−B interface, is naturally expressed as a product of three factors:

$$Z_A^{graft} = \left(\frac{z-1}{e}\right)^{LA - M_{brush}} \left\{\frac{1}{\beta R^3} e^{-3L^2/2R^2}\right\}^{M_{brush}} (R^2 L)^{M_{brush}} \tag{E1}$$

where $\beta \equiv (2\pi/3)^{3/2}$. The first factor is the partition function for an unstretched "grafted melt" of volume LA, derived in Appendix F (eq F3). The second factor represents a normalized Gaussian entropy loss due to the fact that each chain is stretched in the x direction with length of order L. The third factor corresponds to the volume available to the nongrafted ends, each of which may lie anywhere within the brush in the x direction,[35] and roughly within R of the graft point in directions parallel to the interface. A similar expression follows for Z_B^{graft}, the partition function of the grafted half B brush.

Now we imagine bringing the two half-brushes together (keeping the graft points fixed), allowing them to mix with one another. Mixing will occur in the narrow interfacial region only, the Flory χ parameter being sufficiently large that the A and B polymers are immiscible.[1] Helfand and Tagami[18] and Semenov[35] have shown that the resultant interfacial free energy of mixing is given by

$$\frac{F_{AB}^{interface}}{T} \approx \frac{A}{a^2}\chi^{1/2} \qquad \phi_A(x) = \frac{1}{2}[1 + \tanh(x/h_0)] \tag{E2}$$

where $\phi_A(x)$ is the equilibrium A monomer volume fraction profile ($\phi_B = 1 - \phi_A$) and $h_0 \equiv a/(6\chi^{1/2})$ is the interface width. These expressions are no different from those for *ungrafted* A and B melts since N is so large that the location of the "first" end of each chain is forgotten. Note that all graft points are assumed to be well away from the interface region at this stage.

To complete the construction of the diblock brush, a pair of grafted A and B ends is joined up to form a diblock joint at location $\mathbf{r}$. This entails moving both grafted ends from deep within their respective bulks to $\mathbf{r}$, which may be in the interfacial region. Semenov[35] has shown that if this process is repeated for all grafted end pairs such that the density of diblock joints is $\rho(\mathbf{r})$, then the resultant change in free energy is $-1/2 \int \mathrm{d}^3r\ \rho(\mathbf{r})[\ln \phi_A(r)\ \phi_B(\mathbf{r})]$ where $\phi_A(r)$ and $\phi_B(\mathbf{r})$ are the equilibrium profiles of eq E2. Adding to this the free energy due to translational mobility of the joints, namely $\int \mathrm{d}^3r\ \rho(\mathbf{r})\ln[\rho(\mathbf{r})/e]$, and minimizing the sum with respect to $[\rho(\mathbf{r})]$ (subject to the constraint that the total number of joints is $\int \mathrm{d}^3r\ \rho = A/\Sigma$), one obtains the following total free energy contribution due to joints:

$$\frac{F_{AB}^{joints}}{T} = M_{brush} \ln \frac{a^3}{\pi e \Sigma h_0} \quad \text{(E3)}$$

Clearly, this describes the translational entropy of each of the identical joints which has available to it an effective volume of thickness h_0 and area Σ.

Summing all of the above contributions, the total free energy is $F_{AB}^{brush} = -T \ln(z_A^{graft} Z_B^{graft}) + F_{AB}^{interface} + F_{AB}^{joints}$. One obtains

$$\frac{F_{AB}^{brush}}{T} = 2M_{brush}\left\{(N-1)\ln\frac{e}{z-1} + \frac{3L^2}{2R^2} + \ln\frac{R}{\beta L}\right\} + \frac{A}{a^2}\chi^{1/2} + M_{brush}\ln\frac{a^3}{\pi e \Sigma h_0} \quad \text{(E4)}$$

Finally, it is simple to show that when there are two types of diblocks in the brush, distinguishable from one another but otherwise identical, eq E4 is replaced by

$$\frac{F_{AB}^{brush}(M_{brush}^{temp}, M_{brush}^{perm})}{T} = (M_{brush}^{temp} + M_{brush}^{perm})\left\{(N-1)\ln\frac{e}{z-1} + \frac{3L^2}{2R^2} + \ln\frac{R}{\beta L}\right\} + \frac{A}{a^2}\chi^{1/2} + M_{brush}^{temp}\ln\frac{a^3 M_{brush}^{temp}}{\pi e A h_0} + M_{brush}^{perm}\ln\frac{a^3 M_{brush}^{perm}}{\pi e A h_0} \quad \text{(E5)}$$

Appendix F. Partition Function of Bulk Melt

Consider an incompressible melt of volume V comprising M chains of one type and M' of another type. The two types are mutually distinguishable but otherwise identical and of length N. In a mean field lattice picture the partition function is given by[36]

$$Z_{bulk}(M,M') = \frac{1}{M!M'!}[\tilde{V}(z-1)^{N-1}]^{M+M'}\frac{\tilde{V}!}{\tilde{V}^{\tilde{V}}} \quad \text{(F1)}$$

where $\tilde{V} \equiv V/a^3$ is the number of lattice sites. For each chain, the first monomer can be placed in any of $\tilde{V}$ possible sites and the $N-1$ other monomers are thought of as each having $z-1$ choices where z is the lattice coordination number (this is of course an approximation). Laying down the chains sequentially, in the mean field approximation the probability that any site is free equals the current volume fraction of free sites; $\tilde{V}!/\tilde{V}^{\tilde{V}}$ is the product of all $\tilde{V}$ such factors. Using $\tilde{V}!/\tilde{V}^{\tilde{V}} \approx e^{-\tilde{V}}$ this gives

$$Z_{bulk}(M,M') = \frac{(V/a^3)^{M+M'}}{M!M'!}(z-1)^{(N-1)(M+M')}e^{-V/a^3}$$

$$\frac{V}{a^3} = (M+M')N \quad \text{(F2)}$$

The second relation follows from incompressibility.

Consider now a "grafted melt", that is a melt as above but now one end of every chain is fixed at a given lattice site. We consider the case of all chains of one type ($M' = 0$). Relative to the partition function for the ungrafted melt there are three changes: (1) the $1/M!$ factor is absent (the chains are now distinguishable); (2) the chain end translational entropy factors of $\tilde{V}$ and the site vacancy probability factors for chain ends are absent; (3) the ungrafted monomers now have a reduced volume $V' = V - Ma^3$ available to them. Hence $Z_{bulk}^{grafted} = (z-1)^{(N-1)M}W!/W^W$ where $W \equiv V'/a^3$. This gives

$$Z_{bulk}^{grafted}(M) = \left(\frac{z-1}{e}\right)^{V-M} \qquad V = MN \quad \text{(F3)}$$

References and Notes

(1) de Gennes, P. G. *Scaling Concepts in Polymer Physics*; Cornell University Press: Ithaca, NY, 1985.
(2) de Gennes, P. G. *J. Colloid Interface Sci.* **1987**, *27*, 189.
(3) Zheng, X.; Sauer, B. B.; Van Alsten, J. G.; Schwarz, S. A.; Rafailovich, M. H.; Sokolov, J.; Rubinstein, M. *Phys. Rev. Lett.* **1995**, *74*, 407.
(4) Halperin, A.; Tirrel, M.; Lodge, T. P. *Adv. Polym. Sci.* **1992**, *100*, 31.
(5) Wu, S. *Polymer* **1985**, *26*, 1855.
(6) Okamoto, M.; Inoue, T. *Polym. Eng. Sci.* **1993**, *33*, 175.
(7) Sundararaj, U.; Macosko, C. *Macromolecules* **1995**, *28*, 2647.
(8) Scott, C.; Macosko, C. *J. Polym. Sci., Part B* **1994**, *32*, 205.
(9) Creton, C.; Kramer, E. J.; Hui, C. Y.; Brown, H. R. *Macromolecules* **1992**, *25*, 3075.
(10) Washiyama, J.; Creton, C.; Kramer, E. J.; Xiao, F.; Hui, C. Y. *Macromolecules* **1993**, *26*, 6011.
(11) Gersappe, D.; Irvine, D.; Balazs, A. C.; Liu, Y.; Sokolov, J.; Rafailovich, M.; Schwarz, S.; Peiffer, D. G. *Science* **1994**, *265*, 1072.
(12) Leibler, L. *Makromol. Chem., Macromol. Symp.* **1988**, *16*, 1.
(13) Wang, Z. G.; Safran, S. A. *J. Phys. (Paris)* **1990**, *51*, 185.
(14) Durning, C. J.; O'Shaughnessy, B. *J. Chem. Phys.* **1988**, *88*, 7117.
(15) O'Shaughnessy, B.; Sawhney, U. *Phys. Rev. Lett.* **1996**, *76*, 3444.
(16) Fredrickson, G. H. *Phys. Rev. Lett.* **1996**, *76*, 3440.
(17) Helfand, E.; Tagami, Y. *Polym. Lett.* **1971**, *9*, 741.
(18) Helfand, E.; Tagami, Y. *J. Chem. Phys.* **1972**, *56*, 3592.
(19) Friedman, B.; O'Shaughnessy, B. *Int. J. Mod. Phys. B* **1994**, *8*, 2555.
(20) Doi, M. *Chem. Phys.* **1975**, *11*, 115.
(21) de Gennes, P. G. *J. Chem. Phys.* **1982**, *76*, 3316, 3322.
(22) Friedman, B.; O'Shaughnessy, B. *Europhys. Lett.* **1993**, *23*, 667; *Macromolecules* **1993**, *26*, 5726.
(23) O'Shaughnessy, B. *Phys. Rev. Lett.* **1993**, *71*, 3331; *Macromolecules* **1994**, *27*, 3875.
(24) Doi, M.; Edwards, S. F. *The Theory of Polymer Dynamics*; Clarendon Press: Oxford, 1986.
(25) Formally, since there is an exponentially small (in N) but finite density of A chains in the B bulk (and vice versa) our definition implies $h = \infty$ in the limit $V \to \infty$. Strictly speaking, therefore, one should either take $N \to \infty$ before $V \to \infty$, or alternatively limit the x integration in the definition of h to a finite region about $x = 0$.
(26) Wilemski, G.; Fixman, M. *J. Chem. Phys.* **1974**, *60*, 866, 878.
(27) Friedman, B.; O'Shaughnessy, B. *Phys. Rev. Lett.* **1988**, *60*, 64.
(28) Friedman, B.; O'Shaughnessy, B. *J. Phys. II (Paris)* **1993**, *3*, 1657.
(29) Ma, S. *Modern Theory of Critical Phenomena*; Benjamin Cummings: London, 1976.
(30) Ferry, J. D. *Viscoelastic Properties of Polymers*, 3rd ed.; John Wiley and Sons: New York, 1980.
(31) de Gennes, P. G. *Macromolecules* **1980**, *13*, 1069.
(32) Zhulina, E. B.; Borisov, O. V.; Brombacher, L. *Macromolecules* **1991**, *24*, 4679.
(33) Zhulina, E. B.; Borisov, O. V. *J. Colloid Interface Sci.* **1991**, *144*, 507.
(34) Semenov, A. N. *Macromolecules* **1992**, *25*, 4967.
(35) Semenov, A. N. *Sov. Phys. JETP* **1985**, *61*, 733.
(36) Flory, P. *Principles of Polymer Chemistry*; Cornell University Press: Ithaca, NY, 1971.
(37) A similar conclusion for the closely related problem of surface grafting was reached by Kramer (Kramer, E. J. *Isr. J. Chem.* **1995**, *35*, 49), who found $k \propto e^{-\text{const } N/\Sigma^2}$ in the crowded interface limit.

MA9601171